Saudi Journal of Biological Sciences 27 (2020) 3376–3384

Contents lists available at ScienceDirect

Saudi Journal of Biological Sciences

journal homepage: www.sciencedirect.com

Original article

Antileukemic activity of sulfoxide nutraceutical allicin against THP-1 cells is associated with premature phosphatidylserine exposure in human erythrocytes

Samar A. Sultan [a], Mohammed H. Khawaji [a,b], Jawaher Alsughayyir [c], Mohammad A. Alfhili [d], Hassan S. Alamri [e,f], Bahauddeen M. Alrfaei [g,*]

[a] Department of Medical Laboratory Technology, College of Applied Medical Sciences, King Abdulaziz University, Jeddah, Saudi Arabia
[b] Department of Biochemistry, Faculty of Applied Medical Sciences, University of Jazan, Jizan, Saudi Arabia
[c] Department of Clinical Laboratory Sciences, College of Applied Medical Sciences, King Saud University, Riyadh 11433, Saudi Arabia
[d] Chair of Medical and Molecular Genetics Research, Department of Clinical Laboratory Sciences, College of Applied Medical Sciences, King Saud University, Riyadh 11433, Saudi Arabia
[e] Clinical Laboratory Science Department, College of Applied Medical Sciences, King Saud bin Abdulaziz University for Health Sciences, Riyadh, Saudi Arabia
[f] King Abdullah International Medical Research Centre (KAIMRC), Riyadh, Saudi Arabia
[g] Stem Cell and Regenerative Medicine, King Abdullah International Medical Research Centre (KAIMRC)/King Saud bin Abdulaziz University for Health Sciences, King Abdulaziz Medical City, Ministry of National Guard Health Affairs, Saudi Arabia

ARTICLE INFO

Article history:
Received 3 March 2020
Revised 30 August 2020
Accepted 1 September 2020
Available online 8 September 2020

Keywords:
Allicin
Eryptosis
Phosphatidylserine
Calcium
CK1α

ABSTRACT

Background: Allicin (ACN), a sulfoxide in freshly crushed garlic, is known for its diverse bioactive properties. Among the most notable effects of ACN is its antitumor activity against a wide array of cancer types. Thus, ACN may be a promising anticancer therapeutic. Nevertheless, chemotherapy-induced anemia is a major obstacle in cancer management with a prevalence of up to 70%. Although the pathophysiology behind it remains elusive, a number of medications known to cause anemia in patients have been shown to induce premature programmed cell death in red blood cells (RBCs) known as eryptosis. This study, thus, investigates the anticancer potential of ACN against THP-1 monocytic leukemia cells, its toxic effects on human RBCs, and delineate the underlying biochemical mechanisms.
Methods: Cytotoxicity was detected using the MTT assay, while hemoglobin leakage was used as a surrogate for hemolysis which was photometrically measured. Major eryptotic events were examined using flow cytometry with fluorescent probes. Phosphatidylserine (PS) exposure was detected by Annexin-V-FITC, cytosolic calcium with Fluo4/AM, and reactive oxygen species with H_2DCFDA.
Results: Our results show that ACN induces hemolysis in a dose-dependent fashion, which is significantly abrogated in absence of extracellular calcium. Moreover, ACN stimulates PS exposure, intracellular calcium overload, and oxidative stress. Using small-molecule inhibitors, we demonstrate that the pro-eryptotic activity of ACN is ameliorated in presence of zVAD(OMe)-FMK, SB203580, and D4476.
Conclusion: ACN possesses both hemolytic and eryptotic properties mediated through elevated intracellular calcium levels, oxidative stress, caspase, p38 MAPK, and CK1α.

1. Introduction

Acute myeloid leukemia (AML) is a type of cancer characterized by overgrowth of progenitor blasts in the bone marrow, blood, and other tissues (Dohner et al., 2015). The most common acute leukemia in adults, AML is difficult to treat with significant mortality and morbidity. This is in part due to the molecular diversity of AML which complicates therapeutic interventions. Up to 85% of patients 60 years of age or younger achieve a complete response, compared to only 60% in those over 60. Moreover, chemotherapy-

* Corresponding author at: Stem Cell and Regenerative Medicine, King Abdullah International Medical Research Center (KAMIRC), King Saud Bin Abdulaziz University for Health Sciences, Ministry of National Guard Health Affairs. MailCode 1515; P.O.box 22490, Riyadh 11426, Saudi Arabia.
E-mail address: alrfaeiba@ngha.med.sa (B.M. Alrfaei).
Peer review under responsibility of King Saud University.

Production and hosting by Elsevier

https://doi.org/10.1016/j.sjbs.2020.09.005
1319-562X/

related side effects in the elderly limit median survival to 5–10 months (Dohner et al., 2015, 2010).

Garlic (*Allium sativum* L.) is an extremely popular plant used around the world in a wide array of nutritional preparations. Known for its beneficial health effects, garlic has been used for centuries as a prophylactic and therapeutic alternative (Bayan et al., 2014). In particular, garlic has been prescribed for leprosy, arthritis, gastrointestinal upset, and gynecological disease, among others (Bayan et al., 2014). Of interest, the plant promotes cardiovascular health as shown by its antihypertensive (Rashid and Khan, 1985; Ried et al., 2013a), antilipidemic (Kamanna and Chandrasekhara, 1982; Rahman and Lowe, 2006; Gardner et al., 2001; Ziaei et al., 2001), antiatherogenic (Jain, 1977; Ried et al., 2013b), and antithrombotic (Bordia et al., 1998; Mirhadi et al., 1991; Allison et al., 2012) effects. Moreover, the antitumor activity of garlic has been demonstrated in multiple studies *in vitro* and *in vivo*. For example, allyl sulfide derivatives, enriched in garlic extracts, exert DNA damage and cell death in cancer cells (Capasso, 2013). In both human and murine models, garlic prevented cancer growth in the lung (Capasso, 2013), bladder (Lau et al., 1986), esophagus (Wargovich et al., 1988), skin (Nishino et al., 1989), mammary gland (Amagase and Milner, 1993), prostate (Hsing et al., 2002), liver (Kweon et al., 2003), and colon (Knowles and Milner, 2003).

Allicin (ACN) is an organosulfur, polyphenolic compound present in freshly crushed garlic (Fig. 1A). Previous reports have described the anti-inflammatory, antioxidant, and antitumor properties of ACN in bacterial, plant, and human cells. ACN showed pro-apoptotic and anticancer activity against cervical, colon, colorectal (Bat-Chen et al., 2010), gastric (Park et al., 2005), leukemia, lymphoma (Miron et al., 2008), adenocarcinoma (Huang et al., 2017), and cholangiocarcinoma (Chen et al., 2018) cells, and is thus proposed for the treatment of malignancy.

It is noteworthy that chemotherapy-induced anemia is prevalent in at least 75% of patients undergoing cancer treatment (Visweshwar et al., 2018). Although the pathophysiology underlying it remains difficult to describe, anemia may develop as a consequence to toxicity to red blood cell (RBC; erythrocyte) precursors in the bone marrow, hemolysis of mature, circulating cells, or premature cell death known as eryptosis. Cell shrinkage, membrane phospholipid scrambling, cytosolic calcium overload, oxidative stress, activation of caspase, mitogen-activated protein kinase (MAPK), and casein kinase (CK); energy depletion, and ceramide accumulation represent the major features of eryptotic erythrocytes (Pretorius et al., 2016).

Many chemotherapeutic agents known to cause anemia in patients, such as doxorubicin and sorafenib, have been shown to induce eryptosis (Lang et al., 2006; Lupescu et al., 2012), but the effect of ACN on human RBCs, which represent an excellent, emerging model for toxicological profiling of xenobiotics (Farag and Alagawany, 2018), remains unknown. The current study thus investigates the anticancer role of ACN against THP-1 cells, a representative model of AML-M3 subtype according to the French-American-British (FAB) classification, and the potential toxicity of ACN on erythrocytes along with the associated molecular mechanisms.

2. Materials & methods

2.1. Blood collection and RBC isolation

This study was approved by the Institutional Review Board of the College of Medicine at King Saud University (Project No. E-20-4544). Blood samples from healthy volunteers were obtained by venipuncture in lithium heparin vacutainer tubes. Erythrocytes were isolated from blood aliquots by density gradient centrifugation at 3000 RPM for 20 min at 20 °C and resuspended in 0.9% NaCl saline solution at a ratio of 1:1 (Alfhili et al., 2019a, Alfhili et al., 2019b).

2.2. Chemicals and reagents

ACN was obtained from Solarbio Life Science (Beijing, China). A 20 mM stock solution of ACN was prepared by dissolving 20 mg of ACN in 6.0 ml of dimethylsulfoxide (DMSO). RPMI-1640 medium, fetal bovine serum (FBS), antibacterial-antimycotic mixture, Hank's balanced salt solution (HBSS), calcium-free HBSS, Annexin-V-FITC, Fluo4/AM, 2′,7′-dichlorodihydrofluorescein diacetate (H_2DCFDA), zVAD(OMe)-FMK (zVAD), SB203580 (SB), and D4476 were purchased from Solarbio. All dyes and inhibitors were dissolved in DMSO to prepare stock solutions of 100 mM.

2.3. Cell culture

THP-1 acute monocytic leukemia cells were maintained in a humidified incubator (37 °C, 5% CO_2) and grown in RPMI-1640 medium supplemented with 10% FBS and 1% antibacterial-antimycotic mixture.

2.4. Cytotoxicity

Cell viability was assayed with CellTiter-Glo® Luminescent Cell Viability Assay (Promega, Madison, Wisconsin, United States) according to the manufacturer's instructions. Briefly, THP-1 cells, with and without 10–100 μM ACN, were seeded in an opaque-walled, 96-well plate at 10,000 cells/well for 24 h, an equal volume of the CellTiter-Glo® reagent was added to each well, and luminescence was finally recorded using VersaMax™ ELISA microplate reader (Molecular Devices, San Jose, CA, USA).

2.5. Hemolysis

Control and experimental RBCs were pelleted by centrifugation at 13,000 × g for 1 min at 20 °C and the supernatant was assayed for hemoglobin content by measuring light absorbance at 405 nm on a VersaMax™ ELISA microplate reader. Cells suspended in distilled water represented 100% hemolysis and ACN-induced hemolysis was derived as a percentage of lysed cells relative to total hemolysis as follows (Alfhili et al., 2019a, Alfhili et al., 2019b):

$$\%\ Hemolysis = \frac{ACN\ induced\ hemoglobin\ release}{water\ induced\ hemoglobin\ release} \times 100$$

2.6. Phosphatidylserine (PS) exposure

A homogeneous 50 μl aliquot of control and treated RBCs was washed and resuspended in 150 μl of 1% Annexin staining solution and incubated at room temperature in the dark for 10 min. Cells were then examined with FACSCanto™ II (Betcon-Dickinson, Franklin Lakes, NJ, USA) at an excitation and emission wavelengths of 488/530 nm, respectively (Alfhili et al., 2019a, 2019b).

2.7. Intracellular calcium

Homogeneous 50 μl aliquots of control and treated RBCs were washed and resuspended in 150 μl of 5 μM Fluo4 staining solution and incubated at 37 °C in the dark for 30 min. Following repeated washing to remove excess dye, cells were subjected to FACS analysis at 488/530 nm excitation and emission spectra (Alfhili et al., 2019a, 2019b).

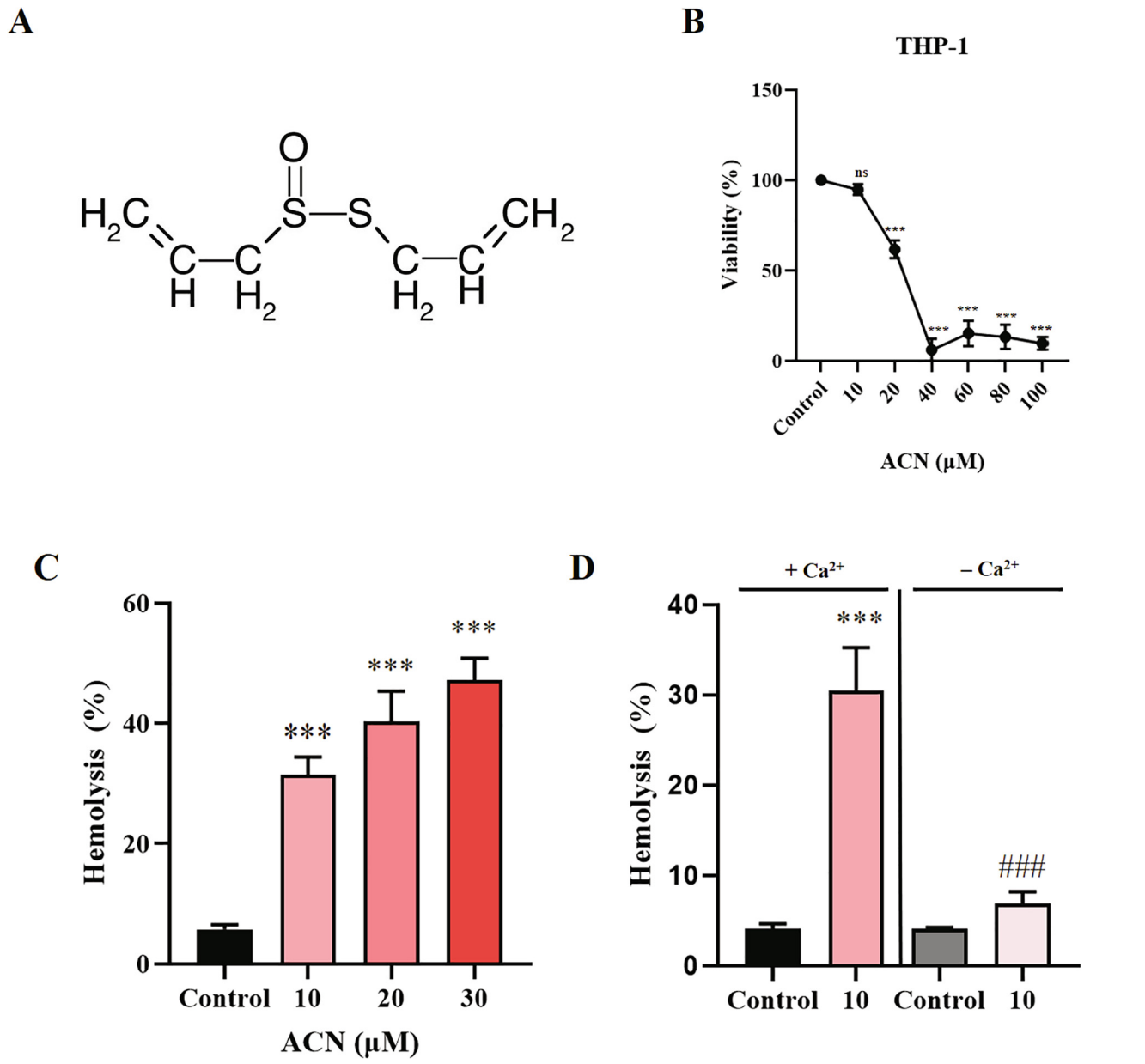

Fig. 1. Cytotoxicity of ACN to THP-1 cells and RBCs. (A) ACN molecular structure. (B) Cells were treated with the vehicle control or with 10–100 μM ACN for 24 h at 37 °C and cytotoxicity was assessed based on the MTT assay. (C) Arithmetic means ± SEM (n = 9) of ACN-induced dose-dependent hemolysis. Cells were treated with the vehicle control or with ACN at 10–30 μM for 24 h at 37 °C and hemolysis was assessed based on hemoglobin release in the medium. (D) Effect of extracellular calcium removal on ACN-induced hemolysis. Cells were treated with the vehicle control or with 10 μM ACN, in HBSS or Ca^{2+}-free HBSS, for 24 h at 37 °C, and hemolysis was subsequently measured. ns ($P > 0.05$) indicates insignificant difference from control. ***($P < 0.001$) indicates significant difference from control. ###($P < 0.001$) indicates significant difference from the corresponding condition in presence of calcium (ANOVA).

2.8. Oxidative stress

Homogeneous 50 μl aliquots of control and treated RBCs were washed and resuspended in 150 μl of 10 μM H_2DCFDA staining solution and incubated at 37 °C away from light for 30 min. Cells were washed twice, excited by488-nm blue laser, and fluorescence of emitted light was captured at 530 nm as a reflection of reactive oxygen species (ROS) levels (Alfhili et al., 2019a, 2019b).

2.9. Inhibitor assays

RBCs were either treated with the vehicle, 10 μM ACN, or a combination of 10 μM ACN and 100 μM caspase inhibitor zVAD, 100 μM p38 MAPK inhibitor SB, or 20 μM CK1α inhibitor D4476, and incubated for 24 h at 37 °C before PS exposure was measured as described earlier.

2.10. Statistical analysis

Data are represented as means ± S.E.M. of triplicate measurements obtained from three independent experiments. To control for individual variation and differential susceptibility of cells, autologous RBCs served as baseline control for each experiment. Multiple means were analyzed by one-way ANOVA and a cutoff P value of < 0.05 was used for statistical significance.

3. Results:

3.1. ACN is cytotoxic to THP-1 cells dose-dependently

First we aimed to show the antitumor potential of ACN against THP-1 leukemia cells. To this end, cells were treated with the vehicle control or 10–100 μM ACN for 24 h and cell viability was assessed by the MTT assay. As shown in Fig. 1B, ACN exerted a dose-dependent cell death significant at 20 μM ACN and beyond. This indicates that ACN possesses antileukemic activity.

3.2. ACN induces dose-dependent hemolysis

In order to assess the hemolytic properties of ACN, RBCs were treated with either the vehicle control or with antitumor levels of ACN (10–30 μM) for 24 °C at 37 °C, and hemoglobin leakage was spectrophotometrically measured as a surrogate for cell death. Fig. 1C shows that ACN caused significant hemolysis at all concentrations tested which reflects disrupted cell membrane integrity. Furthermore, we examined the participation of extracellular calcium in ACN-induced hemolysis. To this end, cells were treated with either the vehicle control or with 10 μM ACN, in HBSS and calcium-free HBSS, and hemoglobin release was again measured. Our results reveal that calcium entry seems to be essential to ACN-induced hemolysis, as removal of extracellular calcium abrogated cell death (Fig. 1D). Thus, dysregulated activity of calcium channels may play a role in hemolysis caused by ACN.

3.3. ACN stimulates phosphatidylserine externalization

Eryptotic cells lose membrane phospholipid asymmetry as PS is externalized to the outer membrane leaflet. Eryptosis was therefore determined by Annexin-V-FITC fluorescence following incubation of RBCs in presence and absence of 10–30 μM ACN for 24 h at 37 °C. Fig. 2C depicts the percentage of cells bound to Annexin, which shows a statistically significant increase at all concentrations tested. Therefore, ACN stimulates eryptosis as evident by PS exposure.

3.4. ACN-induced eryptosis is not associated with cell shrinkage

One of the major events leading up to eryptosis is the activation of calcium-dependent potassium channel. As the channel opens secondary to calcium overload, potassium chloride and water efflux leads to cell shrinkage and death. To estimate cell size, forward scatter (FSC) of control and experimental cells (10–30 μM ACN) was measured, and as shown in Fig. 3C no significant differences in mean FSC among control and ACN-treated cells were found. Similarly, the percentage of enlarged and shrunk cells, as depicted in Fig. 3D and E, respectively, was not statistically significant. These observations seem to indicate that ACN-induced eryptosis is not associated with cell shrinkage.

3.5. ACN elevates intracellular calcium levels

Calcium is a major trigger of cell death, and eryptotic cells display elevated cytosolic calcium levels. Fluo4 fluorescence was used to measure calcium content of control and experimental cells (10–30 μM) following incubation with and without ACN for 24 h at 37 °C. The results in Fig. 4C suggest that ACN caused cell death through elevated intracellular calcium. Moreover, ACN caused a dose-dependent increase in the percentage of cells with elevated calcium, as shown in Fig. 4D. Collectively, ACN causes premature eryptosis, at least in part, through calcium signaling.

Because scramblase is calcium-dependent, it is therefore of interest to examine the importance of calcium availability to ACN-induced PS exposure. The percentage of control and experimental cells (10 μM ACN) was determined following incubation for 24 h at 37 °C with and without extracellular calcium. As seen in Fig. 6E, calcium removal did not significantly influence PS

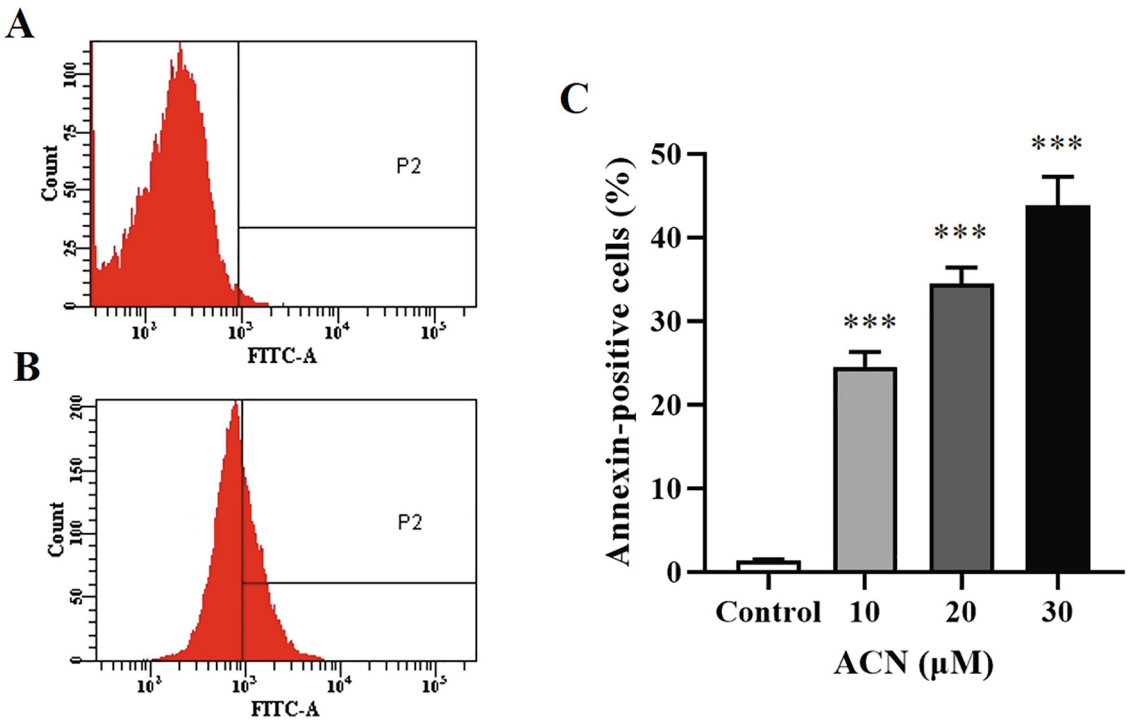

Fig. 2. ACN induces PS exposure. (A) Representative histogram of Annexin-V-FITC fluorescence of control cells. (B) Representative histogram of Annexin-V-FITC fluorescence of cells treated with 30 μM ACN. (C) Arithmetic means ± SEM (n = 9) of ACN-induced dose-dependent PS exposure. Cells were treated with the vehicle control or with ACN at 10–30 μM for 24 h at 37 °C and PS exposure was detected by Annexin-V-FITC staining. ***(P < 0.001) indicates significant difference from control (ANOVA).

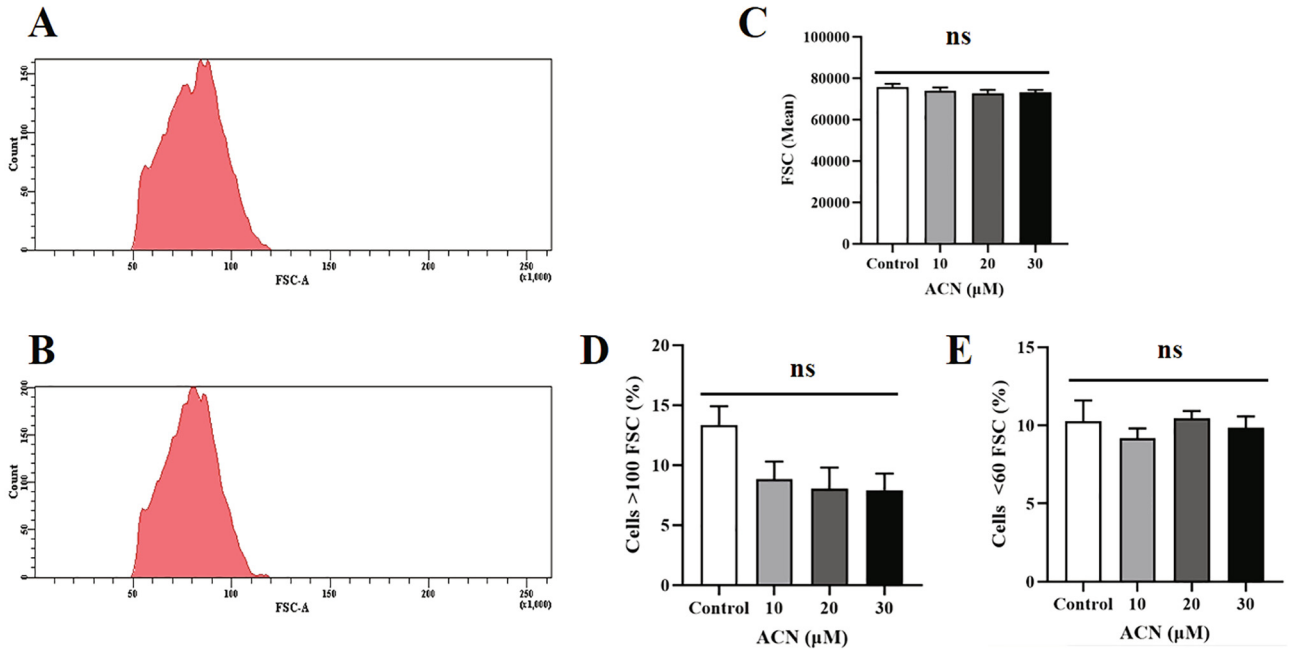

Fig. 3. Effect of ACN on FSC. (A) Representative histogram of FSC of control cells. (B) Representative histogram of FSC of cells treated with 30 μM ACN. (C) Arithmetic means ± SEM (n = 9) of FSC. (D) Arithmetic means ± SEM (n = 9) of the percentage of cells showing a FSC mean value of < 60. (E) Arithmetic means ± SEM (n = 9) of the percentage of cells showing a FSC mean value of > 100. Cells were treated with the vehicle control or with ACN at 10–30 μM for 24 h at 37 °C and cell size was estimated from FSC. ns (P > 0.05) indicates insignificant difference from control (ANOVA).

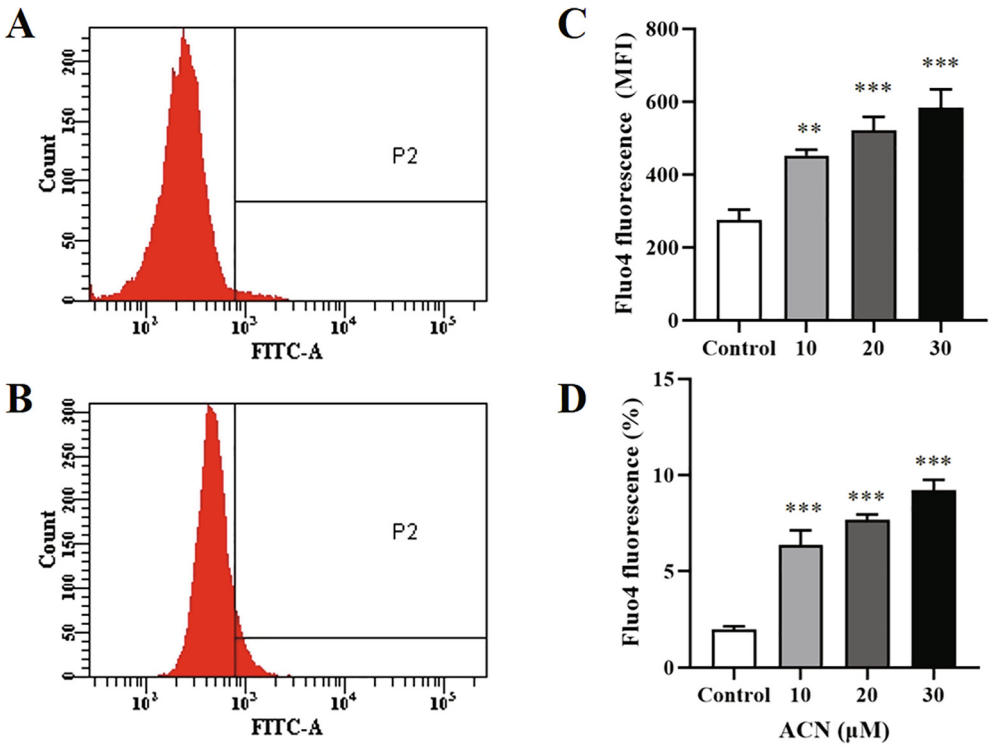

Fig. 4. ACN elevates cytosolic calcium. (A) Representative histogram of Fluo4 fluorescence of control cells. (B) Representative histogram of Fluo4 fluorescence of cells treated with 30 μM ACN. (C) Arithmetic means ± SEM (n = 9) of ACN-induced dose-dependent calcium overload. (D) Arithmetic means ± SEM (n = 9) of the percentage of cells with increased Fluo4 fluorescence. Cells were treated with the vehicle control or with ACN at 10–30 μM for 24 h at 37 °C and cytosolic calcium was measured by Fluo4/AM staining. **(P < 0.01) and ***(P < 0.001) indicate significant difference from control (ANOVA).

externalization, which suggests the possible involvement of other mechanisms. Furthermore, given the increase in calcium levels, we were prompted to examine whether or not it is secondary to extracellular calcium influx. To test this possibility, control and

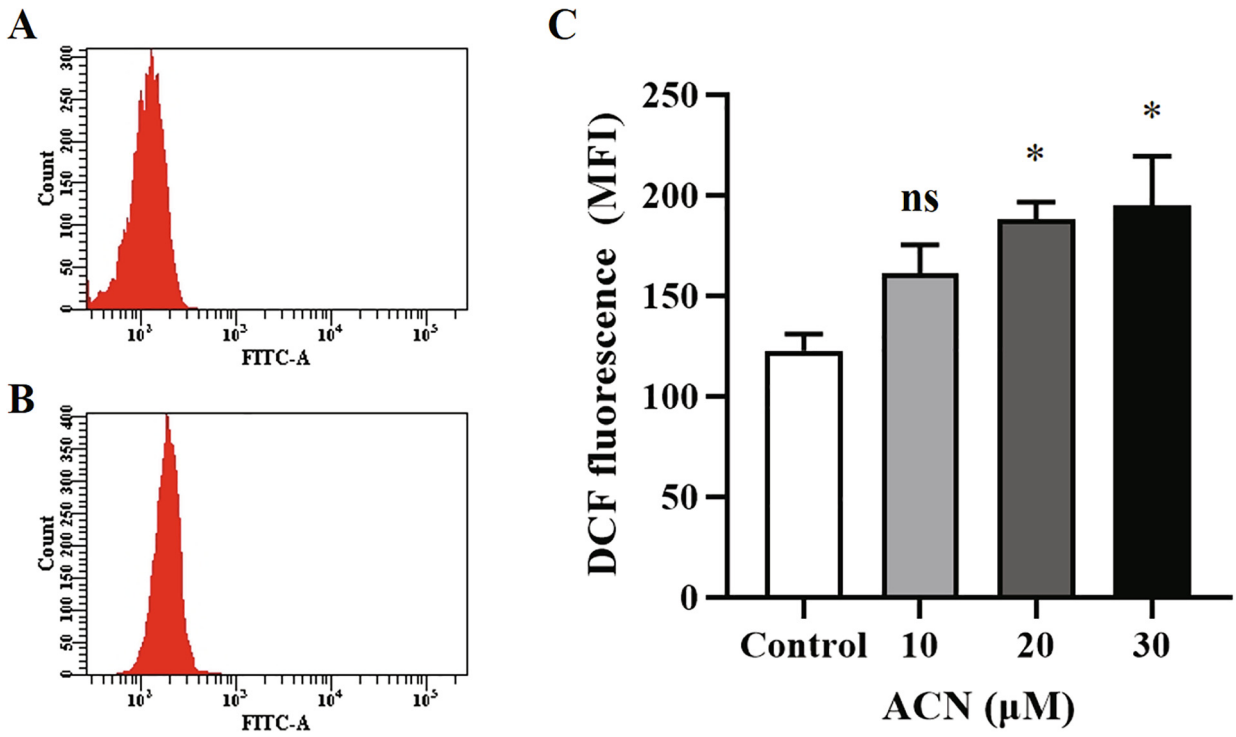

Fig. 5. ACN increases ROS levels. (A) Representative histogram of DCF fluorescence of control cells. (B) Representative histogram of DCF fluorescence of cells treated with 30 μM ACN. (C) Arithmetic means ± SEM (n = 9) of ACN-induced dose-dependent ROS increase. Cells were treated with the vehicle control or with ACN at 10–30 μM for 24 h at 37 °C and ROS were quantified by H2DCFDA staining. *(P < 0.05) indicates significant difference from control (ANOVA).

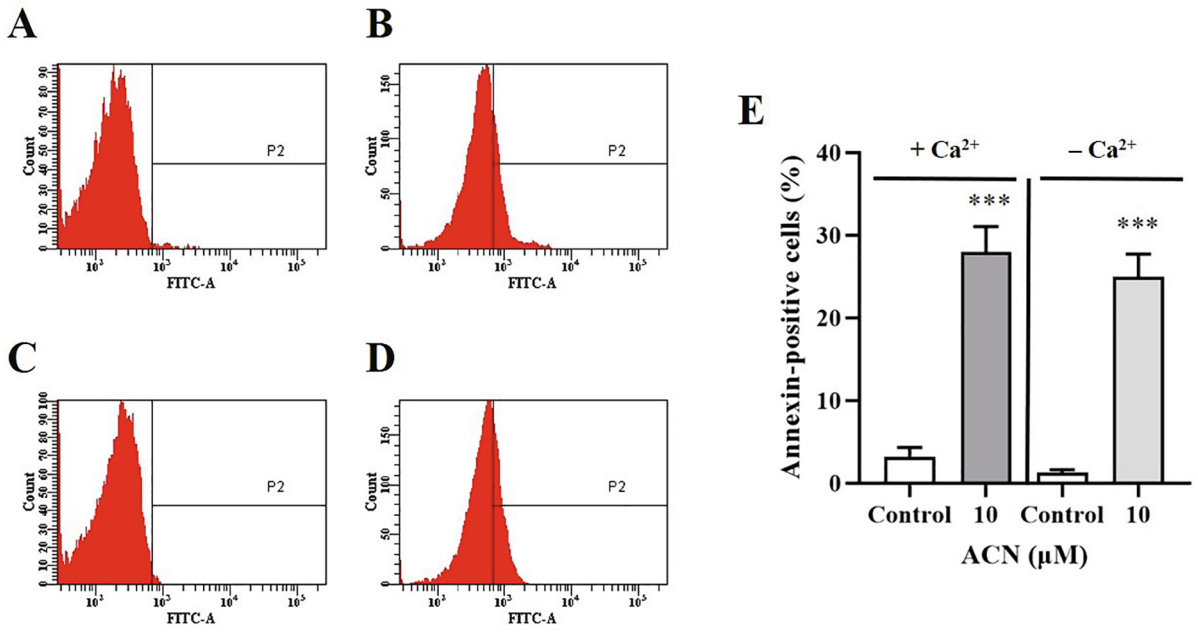

Fig. 6. Effect of extracellular calcium availability on ACN-induced PS exposure. (A) Representative histogram of Annexin-V-FITC fluorescence of control cells. (B) Representative histogram of Annexin-V-FITC fluorescence of cells treated with 10 μM ACN. (C) Representative histogram of Annexin-V-FITC fluorescence of control cells in Ca^{2+}-free HBSS. (D) Representative histogram of Annexin-V-FITC fluorescence of cells treated with 10 μM ACN in Ca^{2+}-free HBSS. (E) Arithmetic means ± SEM (n = 9) of ACN-induced PS exposure in presence and absence of extracellular Ca^{2+}. Cells were treated with the vehicle control or with 10 μM ACN in HBSS or Ca^{2+}-free HBSS for 24 h at 37 °C and PS exposure was detected by Annexin-V-FITC staining. ***(P < 0.001) indicates significant difference from control (ANOVA).

experimental cells (10–30 μM ACN) were incubated in HBSS and calcium-free HBSS for 24 h at 37 °C, and Fluo4 fluorescence was similarly measured. As shown in Fig. 7E, Fluo4 fluorescence was not significantly different in presence and absence of extracellular calcium, which suggests that cytosolic calcium elevation was not caused by calcium entry into the cell.

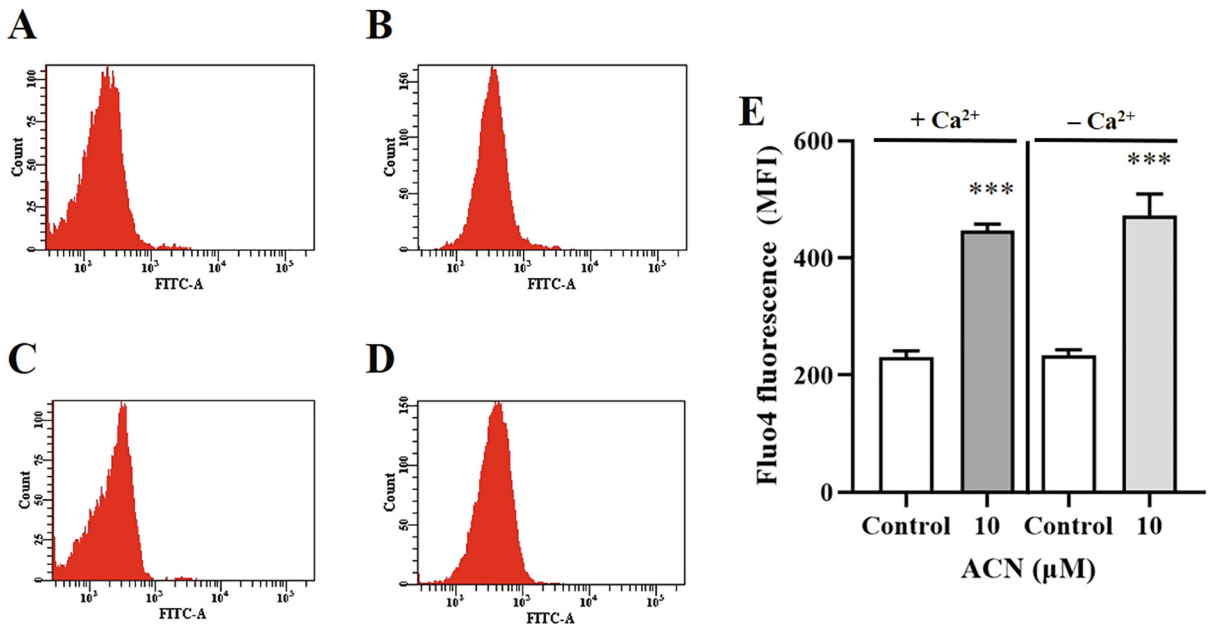

Fig. 7. Effect of extracellular calcium removal on ACN-induced cytosolic calcium elevation. (A) Representative histogram of Fluo4 fluorescence of control cells. (B) Representative histogram of Fluo4 fluorescence of cells treated with 10 μM ACN. (C) Representative histogram of Fluo4 fluorescence of control cells in Ca^{2+}-free HBSS. (D) Representative histogram of Fluo4 fluorescence of cells treated with 10 μM ACN in Ca^{2+}-free HBSS. (E) Arithmetic means ± SEM (n = 9) of ACN-induced intracellular calcium elevation in presence and absence of extracellular Ca^{2+}. Cells were treated with the vehicle control or with 10 μM ACN in HBSS or Ca^{2+}-free HBSS for 24 h at 37 °C and cytosolic calcium was measured by Fluo4 staining. ***($P < 0.001$) indicates significant difference from control (ANOVA).

3.6. ACN promotes ROS generation

Redox balance is integral to cellular survival and oxidative stress is a recognized hallmark of programmed cell death. We investigated whether or not ACN-induced cell death is mediated through disturbances in redox status. To this end, control and experimental cells (10–30 μM) were incubated for 24 h at 37 °C and DCF fluorescence was assessed as a measure of intracellular ROS. Fig. 5C indicates that ACN leads to ROS overproduction, reaching statistical significance at 20 and 30 μM. Therefore, ACN induces premature RBC death through oxidative stress.

3.7. Caspase, p38 MAPK and CK1α are essential for ACN-induced PS exposure

A number of signaling pathways have been identified as modulators of erythrocyte death and survival, including caspases, p38 MAPK, and CK1α, among others. We used small-molecule inhibitors to evaluate the role of key signaling mediators in ACN-induced PS exposure. To this end, cells were treated for 24 h at 37 °C with the vehicle control, 10 μM ACN, or a combination of 10 μM ACN and 100 μM caspase inhibitor zVAD, 100 μM p38 MAPK inhibitor SB, or 20 μM CK1α inhibitor D4476. Fig. 8F demonstrates that while ACN significantly enhanced the percentage of cells bound to Annexin-V, inhibition of caspase, p38 MAPK, and CK1α significantly decrease Annexin-V-positive cells. These three pathways are therefore likely to be essential for the full eryptotic activity of ACN.

4. Discussion:

ACN is an active ingredient in garlic that has garnered enormous interest among researchers for its diverse bioactive properties. This report identifies ACN as antileukemic against THP-1 cells, and reveals a novel activity which is the stimulation of eryptosis. The concentrations required for ACN to induce eryptosis are parallel to those showing anticancer activity (Huang et al., 2017; Chen et al., 2018), which may preclude the clinical utility of the compound.

Chemotherapy-induced anemia may, at least in theory, result from direct cell hemolysis, as demonstrated by ACN in the current study (Fig. 1C). Oxidative damage caused by extravascular hemoglobin is implicated in a variety of conditions including cardiovascular, neurological, and renal disease (Alfhili et al., 2019b). It is interesting to note that our data suggest that ACN-induced hemolysis is secondary to calcium influx from the medium, as shown in Fig. 1D. Accordingly, ACN may cause excessive activity in calcium channels, intracellular calcium overload, and eventual membrane rupture.

The ability of ACN to stimulate PS externalization (Fig. 2) complements previous reports of its pro-apoptotic activity in nucleated cells (Bayan et al., 2014). The presence of PS on the outer membrane leaflet serves as a binding site for phagocytes, which primes RBCs for removal from the circulation before intravascular hemolysis ensues. Likewise, the prolonged presence of eryptotic RBCs in the circulation favors thrombosis due to loss of membrane deformability and compromised rheology (Walker et al., 2014; Pretorius, 2018). Thus, eryptosis may be perceived as a defense mechanism that ensures the continuous disposal of aged, damaged, or infected cells.

Our data also identifies calcium signaling as an important mediator of ACN-induced eryptosis (Fig. 4). Nevertheless, unlike hemolysis, neither PS exposure nor cytosolic calcium was significantly influenced by calcium withdrawal from the extracellular space, an observation indicating the involvement of mechanisms downstream of calcium (Figs. 7E & 8E). Of note, calcium plays a major role in cell survival as it regulates scramblase activity and is hence responsible for maintaining the asymmetry of the cell membrane. Also, increased intracellular calcium opens up potassium channels leading to potassium chloride loss along with water, due to membrane hyperpolarization, and eventual cell death (Lang et al., 2012). Interestingly, although calcium is a pivotal element of eryptosis,

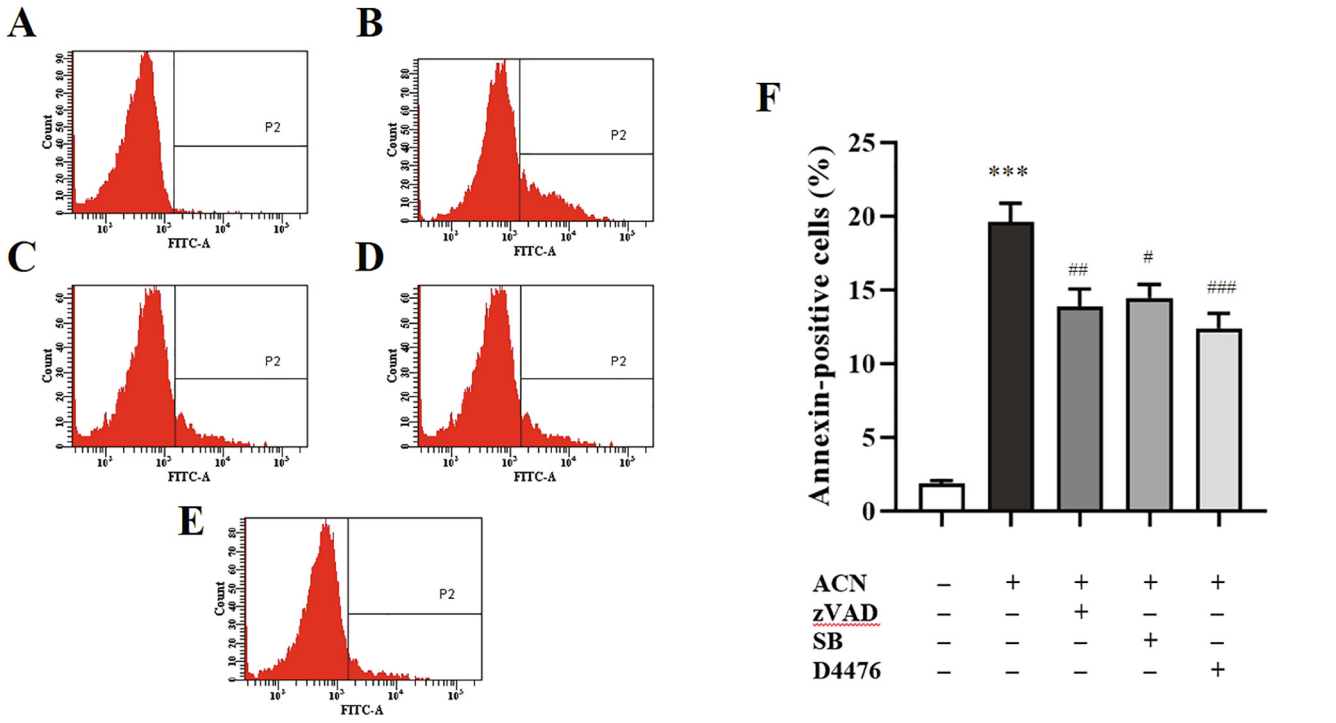

Fig. 8. Caspase, p38 MAPK, and CK1α are essential for ACN-induced PS exposure. (A) Representative histogram of Annexin-V-FITC fluorescence of control cells. (B) Representative histogram of Annexin-V-FITC fluorescence of cells treated with 10 μM ACN. (C) Representative histogram of Annexin-V-FITC fluorescence of cells cotreated with 100 μM zVAD and 10 μM ACN. (D) Representative histogram of Annexin-V-FITC fluorescence of cells treated with 100 μM SB and 10 μM ACN. (E) Representative histogram of Annexin-V-FITC fluorescence of cells treated with 20 μM D4476 and 10 μM ACN. (F) Arithmetic means ± SEM (n = 9) of ACN-induced dose-dependent PS exposure. Cells were treated with the vehicle control or with ACN at 10 μM, in presence and absence of zVAD, SB, or D4476, for 24 h at 37 °C and PS exposure was detected by Annexin-V-FITC staining. $^{***}(P < 0.001)$ indicates significant difference from control. $^{\#\#}(P < 0.01)$, and $^{\#\#\#}(P < 0.001)$ indicate significant difference from ACN-treated cells (ANOVA).

calcium levels were reduced in eryptotic cells treated with the antitumor drug regorafenib (Zierle et al., 2016).

Previous reports have discerned both pro- and antioxidant properties of ACN. In particular, the compound was shown to protect against oxidative damage caused by lipopolysaccharide, acrylamide, and hydrogen peroxide, among others (Zhang et al., 2017; Hong et al., 2019; Tu et al., 2016). On the other hand, ACN increased oxidized glutathione levels and caused cell death in a panel of human and mouse cell lines (Gruhlke et al., 2016). In RBCs, our data show that ACN acts as a pro-oxidant (Fig. 5), which may contribute to hemolysis (Fig. 1) and be the trigger behind membrane scrambling (Fig. 2). This is comprehensible considering that oxidative stress is a hallmark of both hemolysis and eryptosis. ROS accumulation lead to opening of calcium channels as well as caspase signaling (Bissinger et al., 2019). Indeed, blocking caspase activity with specific inhibitor zVAD significantly attenuated ACN-induced PS exposure (Fig. 8C & E), an event possibly implicating an ROS-caspase-PS axis. Again, as is the case with calcium, while oxidative injury caused by ACN resembles that of steroid diosgenin, alkaloid fascaplysin (Mischitelli et al., 2016a, Mischitelli et al., 2016b) and many others, we have previously shown, however, that both insect repellent *N*,*N*-Diethyl-3-methylbenzamide and antimicrobial triclosan seem to elicit eryptosis independent of redox imbalance (Alfhili et al., 2019a, Alfhili et al., 2019b).

Beside caspase, our inhibitor studies further identified the participation of p38 MAPK (Fig. 8E). Cells respond to stress stimuli, either chemical or osmotic, by activating p38 which in turn signals for eryptosis (Boulet et al., 2018) possibly upstream of calcium (Gatidis et al., 2011). We have previously shown that triclosan induces p38-dependent eryptosis (Alfhili et al., 2019b) in a similar fashion to cryptanoshinone (Bissinger et al., 2014) and other compounds. Our results also suggest that CK1α may be essential to ACN-induced PS translocation which was significantly reversed in presence of D4476 (Fig. 8E). This kinase is a recognized regulator of eryptosis and seems to act upstream of calcium signaling (Zelenak et al., 2012). Previous compounds, most notably, mammalian target of rapamycin (mTOR) inhibitor temsirolimus (Al Mamun Bhuyan et al., 2017) and retinoid X receptor agonist bexarotene (Al Mamun Bhuyan et al., 2016) similarly cause eryptosis through CK1 α.

5. Conclusions

In conclusion, this report reveals that ACN is cytotoxic to THP-1 cells and induces calcium-dependent hemolysis and eryptosis in human RBCs, which provides a working platform for future *in vivo* investigations. Mechanistic studies showed that ACN elevates intracellular calcium levels, causes oxidative stress, and stimulates caspase, p38 MAPK, and CK1α. Careful consideration of ACN for use in chemotherapy is thus warranted. It is important to mention that inhibitors of eryptosis, especially endogenous compounds, have been identified (Pretorius et al., 2016; Lang and Lang, 2015), and their use with ACN may therefore limit its detrimental effects on RBCs.

Declaration of Competing Interest

The authors declare that they have no known competing financial interests or personal relationships that could have appeared to influence the work reported in this paper.

Acknowledgment

This project was funded by the Deanship of Scientific Research (DSR), King Abdulaziz University, Jeddah, under grant No. (DF-599-290-1441). The authors, therefore, gratefully acknowledge DSR technical and financial support.

References

Al Mamun Bhuyan, A., Bissinger, R., Cao, H., Lang, F., 2016. Triggering of suicidal erythrocyte death by bexarotene. Cell. Physiol. Biochem. 40, 1239–1251.
Al Mamun Bhuyan, A., Cao, H., Lang, F., 2017. Triggering of eryptosis, the suicidal erythrocyte death by mammalian target of rapamycin (mTOR) inhibitor temsirolimus. Cell. Physiol. Biochem. 42, 1575–1591.
Alfhili, M.A., Nkany, M.B., Weidner, D.A., Lee, M.H., 2019a. Stimulation of eryptosis by broad-spectrum insect repellent N, N-Diethyl-3-methylbenzamide (DEET). Toxicol. Appl. Pharmacol. 370, 36–43.
Alfhili, M.A., Weidner, D.A., Lee, M.H., 2019b. Disruption of erythrocyte membrane asymmetry by triclosan is preceded by calcium dysregulation and p38 MAPK and RIP1 stimulation. Chemosphere 229, 103–111.
Allison, G.L., Lowe, G.M., Rahman, K., 2012. Aged garlic extract inhibits platelet activation by increasing intracellular cAMP and reducing the interaction of GPIIb/IIIa receptor with fibrinogen. Life Sci. 91, 1275–1280.
Amagase, H., Milner, J.A., 1993. Impact of various sources of garlic and their constituents on 7,12-dimethylbenz[a]anthracene binding to mammary cell DNA. Carcinogenesis 14, 1627–1631.
Bat-Chen, W., Golan, T., Peri, I., Ludmer, Z., Schwartz, B., 2010. Allicin purified from fresh garlic cloves induces apoptosis in colon cancer cells via Nrf2. Nutr. Cancer 62, 947–957.
Bayan, L., Koulivand, P.H., Gorji, A., 2014. Garlic: a review of potential therapeutic effects. Avicenna J. Phytomed. 4, 1–14.
Bissinger, R., Bhuyan, A.A.M., Qadri, S.M., Lang, F., 2019. Oxidative stress, eryptosis and anemia: a pivotal mechanistic nexus in systemic diseases. FEBS J. 286, 826–854.
Bissinger, R., Lupescu, A., Zelenak, C., Jilani, K., Lang, F., 2014. Stimulation of eryptosis by cryptotanshinone. Cell. Physiol. Biochem. 34, 432–442.
Bordia, A., Verma, S.K., Srivastava, K.C., 1998. Effect of garlic (Allium sativum) on blood lipids, blood sugar, fibrinogen and fibrinolytic activity in patients with coronary artery disease. ProstaglandinsLeukot. Essent. Fatty Acids 58, 257–263.
Boulet, C., Doerig, C.D., Carvalho, T.G., 2018. Manipulating eryptosis of human red blood cells: a novel antimalarial strategy?. Front. Cell. Infect. Microbiol. 8, 419.
Capasso, A., 2013. Antioxidant action and therapeutic efficacy of Allium sativum L. Molecules 18, 690–700.
Chen, H., Zhu, B., Zhao, L., Liu, Y., Zhao, F., Feng, J., Jin, Y., Sun, J., Geng, R., Wei, Y., 2018. Allicin inhibits proliferation and invasion in vitro and in vivo via SHP-1-mediated STAT3 signaling in cholangiocarcinoma. Cell. Physiol. Biochem. 47, 641–653.
Dohner, H., Estey, E.H., Amadori, S., Appelbaum, F.R., Buchner, T., Burnett, A.K., Dombret, H., Fenaux, P., Grimwade, D., Larson, R.A., Lo-Coco, F., Naoe, T., Niederwieser, D., Ossenkoppele, G.J., Sanz, M.A., Sierra, J., Tallman, M.S., Lowenberg, B., Bloomfield, C.D., European, L., 2010. Diagnosis and management of acute myeloid leukemia in adults: recommendations from an international expert panel, on behalf of the European LeukemiaNet. Blood 115, 453–474.
Dohner, H., Weisdorf, D.J., Bloomfield, C.D., 2015. Acute myeloid leukemia. N. Engl. J. Med. 373, 1136–1152.
Farag, M.R., Alagawany, M., 2018. Erythrocytes as a biological model for screening of xenobiotics toxicity. Chem. Biol. Interact. 279, 73–83.
Gardner, C.D., Chatterjee, L.M., Carlson, J.J., 2001. The effect of a garlic preparation on plasma lipid levels in moderately hypercholesterolemic adults. Atherosclerosis 154, 213–220.
Gatidis, S., Zelenak, C., Fajol, A., Lang, E., Jilani, K., Michael, D., Qadri, S.M., Lang, F., 2011. p38 MAPK activation and function following osmotic shock of erythrocytes. Cell. Physiol. Biochem. 28, 1279–1286.
Gruhlke, M.C., Nicco, C., Batteux, F., Slusarenko, A.J., 2016. The effects of allicin, a reactive sulfur species from garlic, on a selection of mammalian cell lines. Antioxidants (Basel) 6.
Hong, Y., Nan, B., Wu, X., Yan, H., Yuan, Y., 2019. Allicin alleviates acrylamide-induced oxidative stress in BRL-3A cells. Life Sci. 231, 116550.
Hsing, A.W., Chokkalingam, A.P., Gao, Y.T., Madigan, M.P., Deng, J., Gridley, G., Fraumeni Jr., J.F., 2002. Allium vegetables and risk of prostate cancer: a population-based study. J. Natl. Cancer Inst. 94, 1648–1651.
Huang, L., Song, Y., Lian, J., Wang, Z., 2017. Allicin inhibits the invasion of lung adenocarcinoma cells by altering tissue inhibitor of metalloproteinase/matrix metalloproteinase balance via reducing the activity of phosphoinositide 3-kinase/AKT signaling. Oncol. Lett. 14, 468–474.
Jain, R.C., 1977. Effect of garlic on serum lipids, coagulability and fibrinolytic activity of blood. Am. J. Clin. Nutr. 30, 1380–1381.
Kamanna, V.S., Chandrasekhara, N., 1982. Effect of garlic (Allium sativum linn) on serum lipoproteins and lipoprotein cholesterol levels in albino rats rendered hypercholesteremic by feeding cholesterol. Lipids 17, 483–488.
Knowles, L.M., Milner, J.A., 2003. Diallyl disulfide induces ERK phosphorylation and alters gene expression profiles in human colon tumor cells. J. Nutr. 133, 2901–2906.
Kweon, S., Park, K.A., Choi, H., 2003. Chemopreventive effect of garlic powder diet in diethylnitrosamine-induced rat hepatocarcinogenesis. Life Sci. 73, 2515–2526.
Lang, E., Lang, F., 2015. Triggers, inhibitors, mechanisms, and significance of eryptosis: the suicidal erythrocyte death. Biomed. Res. Int. 2015, 513518.
Lang, E., Qadri, S.M., Lang, F., 2012. Killing me softly - suicidal erythrocyte death. Int. J. Biochem. Cell. Biol. 44, 1236–1243.
Lang, P.A., Huober, J., Bachmann, C., Kempe, D.S., Sobiesiak, M., Akel, A., Niemoeller, O.M., Dreischer, P., Eisele, K., Klarl, B.A., Gulbins, E., Lang, F., Wieder, T., 2006. Stimulation of erythrocyte phosphatidylserine exposure by paclitaxel. Cell. Physiol. Biochem. 18, 151–164.
Lau, B.H., Woolley, J.L., Marsh, C.L., Barker, G.R., Koobs, D.H., Torrey, R.R., 1986. Superiority of intralesional immunotherapy with Corynebacterium parvum and Allium sativum in control of murine transitional cell carcinoma. J. Urol. 136, 701–705.
Lupescu, A., Shaik, N., Jilani, K., Zelenak, C., Lang, E., Pasham, V., Zbidah, M., Plate, A., Bitzer, M., Foller, M., Qadri, S.M., Lang, F., 2012. Enhanced erythrocyte membrane exposure of phosphatidylserine following sorafenib treatment: an in vivo and in vitro study. Cell. Physiol. Biochem. 30, 876–888.
Mirhadi, S.A., Singh, S., Gupta, P.P., 1991. Effect of garlic supplementation to cholesterol-rich diet on development of atherosclerosis in rabbits. Indian J. Exp. Biol. 29, 162–168.
Miron, T., Wilchek, M., Sharp, A., Nakagawa, Y., Naoi, M., Nozawa, Y., Akao, Y., 2008. Allicin inhibits cell growth and induces apoptosis through the mitochondrial pathway in HL60 and U937 cells. J. Nutr. Biochem. 19, 524–535.
Mischitelli, M., Jemaa, M., Almasry, M., Faggio, C., Lang, F., 2016a. Ca2+ entry, oxidative stress, ceramide and suicidal erythrocyte death following diosgenin treatment. Cell. Physiol. Biochem. 39, 1626–1637.
Mischitelli, M., Jemaa, M., Almasry, M., Faggio, C., Lang, F., 2016b. Triggering of suicidal erythrocyte death by fascaplysin. Cell. Physiol. Biochem. 39, 1638–1647.
Nishino, H., Iwashima, A., Itakura, Y., Matsuura, H., Fuwa, T., 1989. Antitumor-promoting activity of garlic extracts. Oncology 46, 277–280.
Park, S.Y., Cho, S.J., Kwon, H.C., Lee, K.R., Rhee, D.K., Pyo, S., 2005. Caspase-independent cell death by allicin in human epithelial carcinoma cells: involvement of PKA. Cancer Lett. 224, 123–132.
Pretorius, E., 2018. Erythrocyte deformability and eryptosis during inflammation, and impaired blood rheology. Clin. Hemorheol. Microcirc. 69, 545–550.
Pretorius, E., du Plooy, J.N., Bester, J., 2016. A comprehensive review on eryptosis. Cell. Physiol. Biochem. 39, 1977–2000.
Rahman, K., Lowe, G.M., 2006. Garlic and cardiovascular disease: a critical review. J. Nutr. 136, 736S–740S.
Rashid, A., Khan, H.H., 1985. The mechanism of hypotensive effect of garlic extract. J. Pak. Med. Assoc. 35, 357–362.
Ried, K., Frank, O.R., Stocks, N.P., 2013a. Aged garlic extract reduces blood pressure in hypertensives: a dose-response trial. Eur. J. Clin. Nutr. 67, 64–70.
Ried, K., Toben, C., Fakler, P., 2013b. Effect of garlic on serum lipids: an updated meta-analysis. Nutr. Rev. 71, 282–299.
Tu, G., Zhang, Y.F., Wei, W., Li, L., Zhang, Y., Yang, J., Xing, Y., 2016. Allicin attenuates H(2)O(2)-induced cytotoxicity in retinal pigmented epithelial cells by regulating the levels of reactive oxygen species. Mol. Med. Rep. 13, 2320–2326.
Visweshwar, N., Jaglal, M., Sokol, L., Zuckerman, K., 2018. Chemotherapy-related anemia. Ann. Hematol. 97, 375–376.
Walker, B., Towhid, S.T., Schmid, E., Hoffmann, S.M., Abed, M., Munzer, P., Vogel, S., Neis, F., Brucker, S., Gawaz, M., Borst, O., Lang, F., 2014. Dynamic adhesion of eryptotic erythrocytes to immobilized platelets via platelet phosphatidylserine receptors. Am. J. Physiol. Cell. Physiol. 306, C291–C297.
Wargovich, M.J., Woods, C., Eng, V.W., Stephens, L.C., Gray, K., 1988. Chemoprevention of N-nitrosomethylbenzylamine-induced esophageal cancer in rats by the naturally occurring thioether, diallyl sulfide. Cancer Res. 48, 6872–6875.
Zelenak, C., Eberhard, M., Jilani, K., Qadri, S.M., Macek, B., Lang, F., 2012. Protein kinase CK1alpha regulates erythrocyte survival. Cell. Physiol. Biochem. 29, 171–180.
Zhang, M., Pan, H., Xu, Y., Wang, X., Qiu, Z., Jiang, L., 2017. Allicin decreases lipopolysaccharide-induced oxidative stress and inflammation in human umbilical vein endothelial cells through suppression of mitochondrial dysfunction and activation of Nrf2. Cell. Physiol. Biochem. 41, 2255–2267.
Ziaei, S., Hantoshzadeh, S., Rezasoltani, P., Lamyian, M., 2001. The effect of garlic tablet on plasma lipids and platelet aggregation in nulliparous pregnants at high risk of preeclampsia. Eur. J. Obstet. Gynecol. Reprod. Biol. 99, 201–206.
Zierle, J., Bissinger, R., Bouguerra, G., Abbes, S., Lang, F., 2016. Triggering of suicidal erythrocyte death by regorafenib. Cell. Physiol. Biochem. 38, 160–172.